PROTEINS: Structure, Function, and Genetics 40:436–442 (2000)

A New Fold in the Scorpion Toxin Family, Associated With an Activity on a Ryanodine-Sensitive Calcium Channel

Amor Mosbah,[1] Riadh Kharrat,[2] Ziad Fajloun,[3] Jean-Guillaume Renisio,[1] Eric Blanc,[1] Jean-Marc Sabatier,[3] Mohamed El Ayeb,[2] and Herve Darbon[1]*

[1]*AFMB, Marseille, France*
[2]*Laboratoire des Venins et Toxines, Institut Pasteur de Tunis, Tunis-Belvédère, Tunisie*
[3]*CNRS UMR 6560-IFR Jean-Roche, Faculté de Mèdecine-Nord, Marseille, France*

ABSTRACT **We determined the structure in solution by ^{1}H two-dimensional NMR of Maurocalcine from the venom of *Scorpio maurus*. This toxin has been demonstrated to be a potent effector of ryanodyne-sensitive calcium channel from skeletal muscles. This is the first description of a scorpion toxin which folds following the Inhibitor Cystine Knot fold (ICK) already described for numerous toxic and inhibitory peptides, as well as for various protease inhibitors. Its three dimensional structure consists of a compact disulfide-bonded core from which emerge loops and the N-terminus. A double-stranded antiparallel β-sheet comprises residues 20–23 and 30–33. A third extended strand (residues 9–11) is perpendicular to the β-sheet. Maurocalcine structure mimics the activating segment of the dihydropyridine receptor II-III loop and is therefore potentially useful for dihydropyridine receptor/ryanodine receptor interaction studies. Proteins 2000;40:436–442.** © 2000 Wiley-Liss, Inc.

Key words: maurocalcine; inhibitor-cystine-knot; ryanodine receptor; dihydropyridine receptor; scorpion toxin

INTRODUCTION

Calcium channels can be classified in various subfamilies that include voltage-gated channels of the L-, N-, P-, Q-, R-, and T-types and ligand-activated calcium entry channels. The latter channels include Inositol-1,4,5-triphosphate and ryanodine receptors present in the sarcoplasmic reticulum. These channels release calcium from intracellular storehouses located in the endoplasmic reticulum. Ryanodyne-sensitive calcium channels are further subdivided into RyR1, RyR2, and RyR3, found respectively in the skeletal muscle, the cardiac muscle, or the brain tissue/epithelial cell. RyR receptors are gated by calcium itself or by allosteric coupling to plasmalemmal voltage-operated calcium channels such as the dihydropyridine receptor.[1] A 138-amino acid cytoplasmic loop between repeats II and III of the α1 subunit of the dihydropyridine receptor interacts with a region of the ryanodine receptor.[2]

Ryanodine receptors have few already characterised specific natural ligands. Besides ryanodyne itself, these ligands are found in the scorpion venoms of *Buthus martensii Karsh* (BmK-PL toxin), *Buthus Imperator* (IpTxi and IpTxa toxins), and very recently in the venom of *Scorpio maurus* (Mca toxin). In vitro electrophysiological experiments based on recordings of single ryanodyne-sensitive calcium type 1 channels incorporated into planar lipid bilayers showed that synthetic Maurocalcine (Mca) potently and reversibly modifies channel gating behaviour by inducing prominent subconductance behaviour.[3] Its primary structure shows high sequence homology with IpTxa toxin which has been demonstrated to mimic the activating segment of the dihydropyridine receptor II-III loop.[4] As no structural information was available concerning these ryanodine-sensitive calcium channel effectors, we solved the solution structure of synthetic Mca to get structural insights of the dihydropyridine receptor/ryanodine receptor interaction.

MATERIALS AND METHODS

Sample Preparation

Maurocalcine was chemically synthesised by the solid phase technique. The half-cystine pairing pattern of synthetic Mca was identified by enzyme-based cleavage and Edman sequencing. The pairing is Cys3-Cys17, Cys10-Cys21, and Cys16-Cys32. The identity of synthetic Mca and natural Mca was assessed by analytical C_{18} reversed-phase HPLC, amino acid analysis after acidolysis, and mass determination by matrix-assisted laser desorption ionisation-time of flight mass spectrometry.[3]

A 5 mM sample of synthetic Mca in 0.5 ml of H_2O/D_2O (90/10 by vol.) at pH 3.0 uncorrected for isotope effects was used for NMR spectra recordings. Amide proton exchange rate was determined after lyophilisation of this sample and dissolution in 100% D_2O.

NMR Spectroscopy

All ^{1}H NMR spectra were recorded on a BRUKER DRX500 spectrometer equipped with a HCN probe and self shielded triple axis gradients. The experiments were performed at 300 K. Two-dimensional spectra were acquired using states-TPPI method[5] to achieve F1 quadrature detection.[6] The spectral width in both dimensions was 6000 Hz, and for all experiments except DQF-COSY, the data size was 2,048 points for t2 and 512 points for t1

*Correspondence to: Herve Darbon, AFMB, CNRS UPR 9039, IFR1, 31, Chemin Joseph-Aiguier, 13402 Marseille CEDEX 20, France. E-mail: herve@afmb.cnrs-mrs.fr

Received 4 January 2000; Accepted 4 April 2000

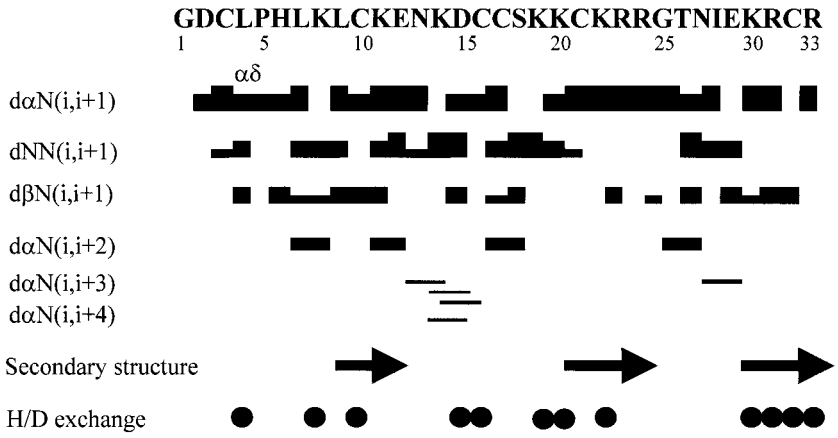

Fig. 1. Amino-acid sequence of Mca and a survey of the sequential assignment: the intensity of sequential nOe's, extracted from NOESY with mixing time of 80 ms are represented by the thickness of the bars. Slowly exchanging amide protons are indicated by closed circles. Extended regions are indicated by arrows.

increments, with 64 transients per experiment. For the DQF-COSY, the data size was 4,096 points for t2 and 512 points for t1. Water suppression was achieved using presaturation during the relaxation delay (1.5s), and during the mixing time in the case of NOESY experiments, or using a watergate 3-9-19 pulse train[7] using a gradient at the magic angle obtained by applying simultaneous x-, y-, and z- gradients prior to detection. NOESY spectra were acquired using mixing times of 80 ms and 120 ms. Clean-TOCSY was performed with a spin locking field strength of 8 kHz and spin lock time of 80 ms. The amide proton exchange experiments were recorded immediately after dissolution of the peptides in D_2O. A series of NOESY spectra with a mixing time of 80 ms were recorded at 300 K, the first one for one hour, followed by spectra of 10 hours each. Furthermore, we obtained the nOe build-up curves by successively recording NOESY's with 50, 150, 200, and 300 ms mixing time in order to check for spin diffusion.

Data Processing

Spectra were processed with Bruker's UXNMR software, running on Silicon Graphics Indy R4400 computer. The matrices were transformed to a final size of 2,048 points in the acquisition dimension and to 1,024 points in the other, except for coupling constant determination for which a 8,192 $\times$ 1,024 matrix was used. The signal was multiplied by a shifted sine bell window in both dimensions prior to a Fourier transform, then a fifth order polynomial baseline correction was applied.

Spectral Analysis

The identification of amino acid spin systems and the sequential assignment were done using the standard strategy described by Wüthrich,[8] applied with a graphical software, XEASY.[9] The comparative analysis of COSY and TOCSY spectra recorded in water gave the spin system signatures of the protein. The spin systems were then sequentially connected using the NOESY spectra.

Experimental Restraints

The integration of NOE data was done by measuring the peak volumes. On the basis of known distances in regular secondary structures ($d_{H\alpha\text{-}H\alpha}$ = 0.23 nm and $d_{HN\text{-}HN}$ = 0.33 nm between two strands of an antiparallel β-sheet), these volumes were translated into upper limits distances by the CALIBA routine[10] of DIANA[11] software. The lower limit was systematically set at 0.18 nm.

The ϕ torsion angles constraints resulted from the $^3J_{HN\text{-}H\alpha}$ coupling constant measurements. They were estimated by the INFIT program.[12] For a given residue, separated NOESY cross peaks with the backbone amide proton in the ω2 dimension were used. Several cross sections through these cross peaks were selected that exhibit a good signal-to-noise ratio. They were added up and only those data points of the peak region that were above the noise level were retained. The left and the right ends of the peak region were then brought to zero intensity by a linear baseline correction. After extending the baseline-corrected peak region with zeros on both sides, which is equivalent to over sampling in the time domain, an inverse Fourier transformation was performed. The value of the $^3J_{HN\text{-}H\alpha}$ coupling constant was obtained from the first local minimum. $^3J_{HN\text{-}H\alpha}$ coupling constants were translated into angle restraints using HABAS from the DIANA package.

The stereospecific assignment was made using the HABAS routine of the DIANA software, on the basis of the upper limits restraints and $^3J_{HN\text{-}H\alpha}$, $^3J_{H\alpha\text{-}H\beta2}$, $^3J_{H\alpha\text{-}H\beta3}$. Pseudoatom corrections were added when stereospecific assignments could not be obtained.

Structure Calculations

Distance geometry calculations were performed with the variable target function program DIANA 2.8. A preliminary set of 1,000 structures was initiated including only intra-residual and sequential upper limit distances. From these, the 500 best were kept for a second round, including medium range distances, and the resulting 250 best for a third one, with the whole set of upper limits restraints, and some additional distance restraints, used to define the disulfide bridges (i.e. $d_{S\gamma,S\gamma}$ 0.21nm, $d_{C\beta,S\gamma}$ and $d_{S\gamma,C\beta}$ 0.31nm). Starting from the 50 best structures, a REDAC strategy[11] was used in a last step, in order to include the dihedral constraints together with the additional distance

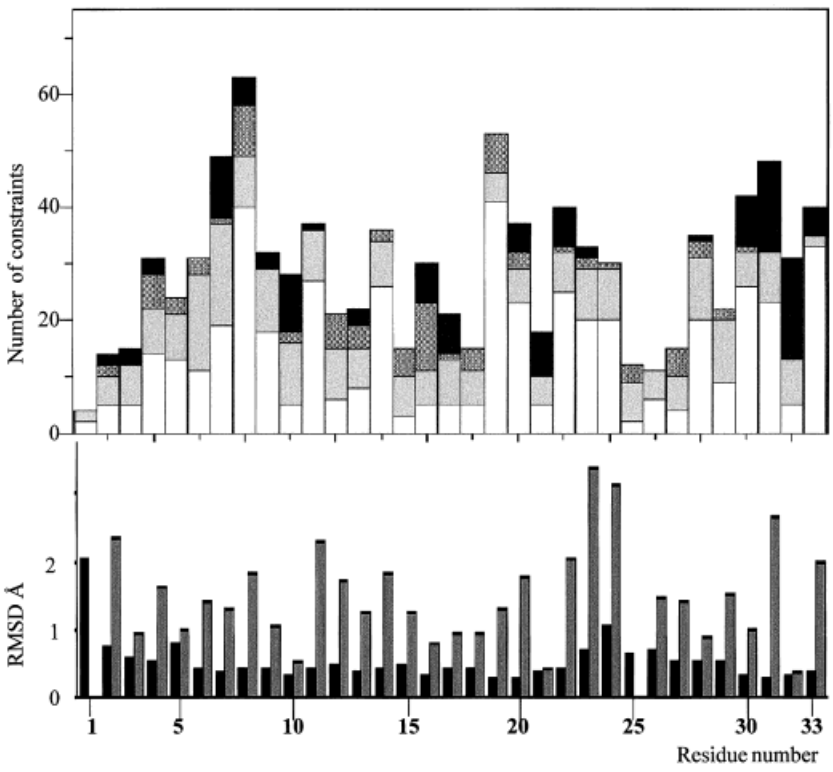

Fig. 2. **Top:** Plot of the number of intra-residue (white bars), sequential (light grey bars), medium range (dark grey), and long range (black bars) nOe. The restraints were classified by Wüthrich's method. **Bottom:** Local value of RMSD calculated on Hα (black bars) and HN (grey bars).

restraints coming from hydrogen bonds. Final energy refinement was achieved by CNS. The visual analysis was done using the TURBO software[13] and the geometric quality of the obtained structures was assessed by PROCHECK 3.3 and PROCHECK-NMR softwares.[14]

Electrostatic Calculations

The electrostatic calculations together with the dipole moments and analysis were done by using the GRASP software[15] running on Silicon Graphics Workstations. The potential maps were calculated with a simplified Poisson-Boltzmann solver,[16] on the basis of an AMBER-derived parameter file.

RESULTS AND DISCUSSION

Structure Calculation

Sequential assignment was obtained by the now standard method first described by Wüthrich.[8] The sequential assignment is summarized on Figure 1. At the end of the sequential assignment procedure, almost all protons were identified and their resonance frequency determined (data deposited in the BMRB bank under the accession number 4696). The structure of Mca was determined by using 483 NOE-based distance restraints (including 231 intra-residue restraints, 137 sequential restraints, 46 medium range restraints, and 69 long range restraints. The distribution of these NOE along the sequence is shown on Figure 2. In addition, 16 hydrogen bond restraints derived from hydrogen exchange data and 29 dihedral angle constraints derived from coupling constants have been included, as well as 9 distance restraints derived from the three disulfide bridges. Altogether, the final experimental set corresponds to 14.6 constraints per residue on the average. The structures were calculated by using a hybrid distance geometry-simulated annealing protocol using DIANA[11] and CNS.[17] The best-fit superimposition of backbone atoms for 25 models gives RMSD values of 0.6 Å for backbone atoms and 1.4 Å if all non-hydrogen atoms are

TABLE I. Structural Statistics of the 25 Best Structures

	RMSD* (Å)	$(DG)^a$	$\langle\overline{DG}\rangle^b$
Backbone ($C, C\alpha, N$)	0.6		
All heavy atoms	1.4		
Energies (kcal/mol)			
Total		42,25	33,10
Bonds		1,67	1,15
Angles		18,43	15,47
Improper		1,44	0,67
Van der Waals		14,88	11,03
nOe		5,77	4,72
Dihedral restraints		$4\ 10^{-2}$	$5{,}47\ 10^{-2}$
RMSD			
Bonds		$1{,}73\ 10^{-2}$ Å	$0{,}15\ 10^{-2}$ Å
Angles		0,33°	0,31°
Improper		0,18°	0,13°
Dihedral		30,3°	29,53°
Cdihedral		0,086°	0,127°
nOe		0,012 Å	0,011 Å

*The RMSD values are calculated with respect to the mean structure.
[a](DG) are the final 25 Mca structures obtained by distance geometry and energy minimisation.
[b]$\langle\overline{DG}\rangle$ is the mean structure obtained by averaging the coordinates of the individual DG structures best fitted to each other.

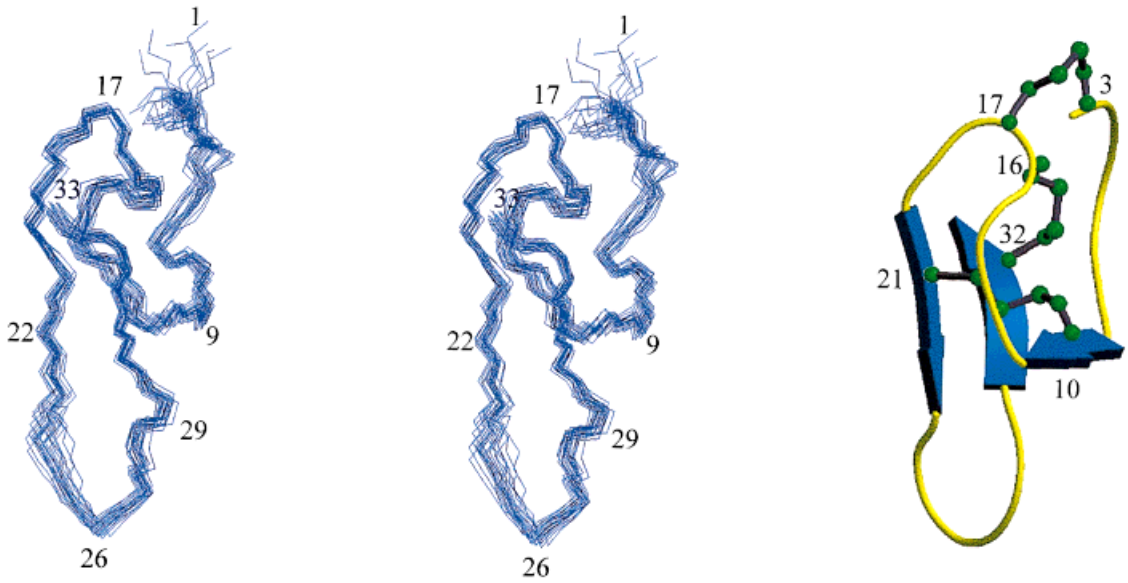

Fig. 3. **Left:** Stereo view of the 25 best molecular Mca structures (only backbone atoms are displayed) superimposed for best fit. **Right:** Molscript ribbon drawing of the averaged minimised Mca structure. The disulfide bridges are in balls and sticks and numbered.

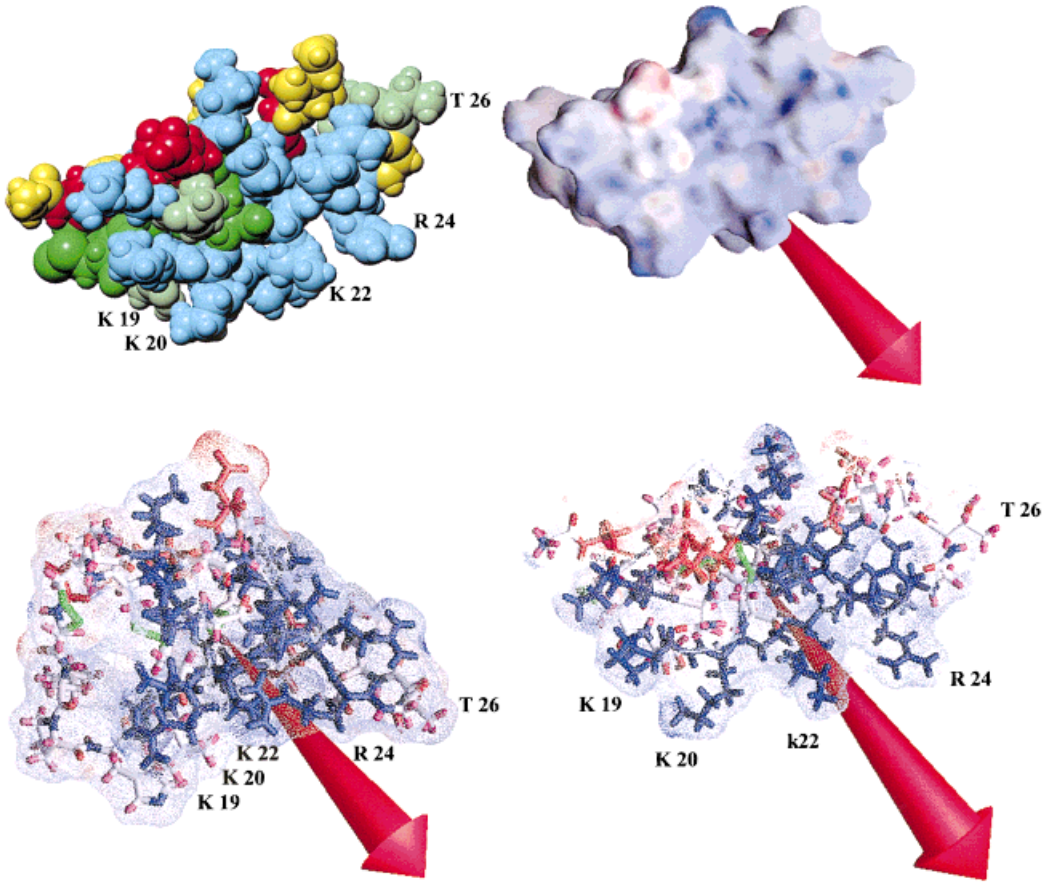

Fig. 4. Electrostatic charge distributions. **Top left:** CPK representation of Mca. Basic residues are in blue and acidic residues in red. **Top right:** molecular surface coloured according to the local electrostatic charges from blue (basic) to red (acidic) and the resulting dipolar moment. **Bottom:** comparison of Mca dipolar moment (right) with Iptxa dipolar moment (left).

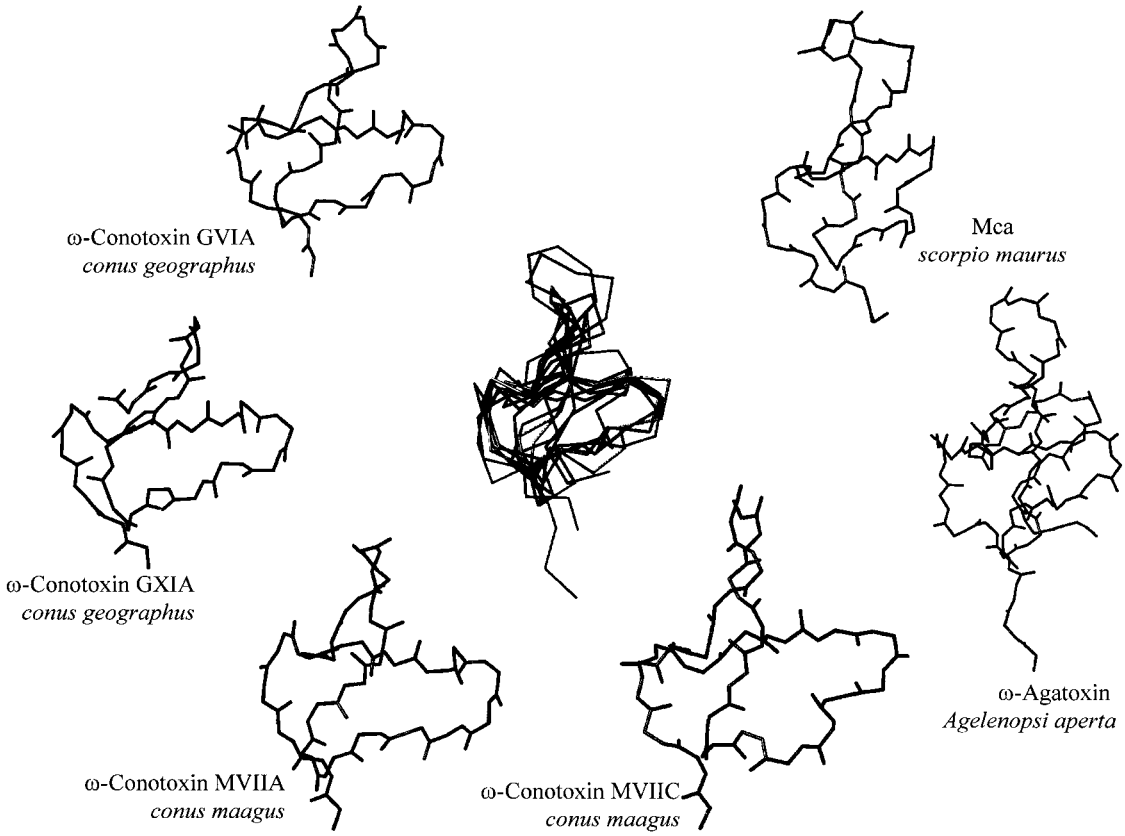

Fig. 5. Conformation of various peptidic effectors of calcium channels and their superimposition for best fit (central image).

included (Fig. 2 and Table I). Analysis of local RMSD values is summarised on Figure 2 and shows that the precision of the calculation is fairly constant all along the sequence. A summary of the structural statistics is given in Table I. All the solutions have good non-bonded contacts and good covalent geometry as evidenced by low values of CNS energy terms. The correlation with the experimental data shows no NOE-derived distance violation greater than 0.2 Å and the analysis of the Ramachandran plot shows (in PROCHECK software nomenclature) 70% of the residues in the most favoured, 30% in the additional, none in the generously allowed regions, nor in the disallowed regions.

Structure Description

The three-dimensional structure (PDB accession code: 1C6W) of Mca consists in a compact disulfide-bonded core, from which several loops and the N-terminus emerge (Fig. 3). The main element of regular secondary structure is a double-stranded antiparallel β-sheet comprising residues 20–23 and 30–33. This structure is stabilized by NH/CO hydrogen bonds involving amide protons from residues 20, 22, 31, and 33. A third peripheral extended strand composed of residues 9–11 is almost perpendicular to the double-stranded antiparallel β-sheet and stabilised by two hydrogen bonds Cys10CO-Cys30NH and Cys30CO-Cys10NH with the 30–33 strand. Amide proton of residue 9 is in fast exchange preserving us to describe the strand 9–11 as a standard β-strand. Other slowly exchanging amide protons, i.e., from residues 4, 15, 16, and 19, are involved in hydrogen bonds with carbonyl oxygens of residues 2, 12, 13, 16 respectively. Mca fold can be classified as *inhibitor cystine knot* fold (ICK) already described in numerous toxic and inhibitory peptides, as well as various protease inhibitors.[18]

Analysis of the overall electrostatic charge distribution (Fig. 4) of Mca reveals a marked anisotropy. This anisotropy can be represented by a dipole moment which emerges from the molecule through a basic-rich surface (Lys19, Lys20, Lys22, Arg23, Arg24, and Arg33) without any acidic residue. Conversely, the opposite surface contains four acidic residues (Asp2, Glu12, Asp15, and Glu29) for only one basic residue (Lys8).

Comparison With Other Calcium Channel Effectors

Mca is the first scorpion toxin known to adopt an ICK fold although his fold has been observed for several other animal toxins from spider and shell venoms (Fig. 5). These ion channel effectors share the same ICK fold although they act with different pharmacological specificities. The μ-conotoxin GIIIA is active on muscle sodium channel[19] as well as conotoxin GS[20] and μ-agatoxin I, whereas κ-cono-

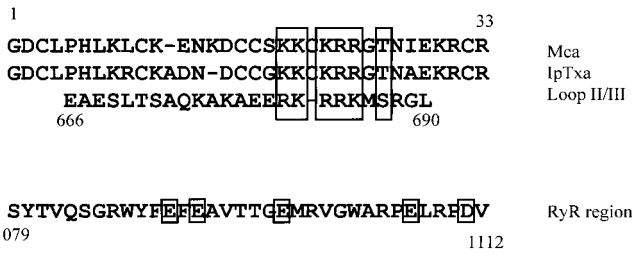

Fig. 6. **Top:** Sequence comparison of Mca with Iptxa and with the loop II/III of the dihydropyridine receptor. The basic residues and the critical Ser/Thr residue are boxed. **Bottom:** Sequence of the ryanodine receptor suggested to be the receptor site of Mca. Acidic residues are boxed.

toxin PVIIA is specific for voltage-gated potassium channel.[21] Some natural toxins have been reported to act on calcium channels: ω-conotoxins MVIIA, MVIIC, GVIA, and GXIA from *Conus geographus*[22] (and references herein) and ω-agatoxin IVA[23] from funnel web spider. Therefore, a same fold can easily support various pharmacological activities.

Mca, which is specific for RyR1, is homologous in sequence to IpTxa from *Pandinus imperator* scorpion venom[24] and therefore the biochemical results obtained when studying the binding properties for it can easily be transferred on the newly determined structure of Mca. Iptxa has been proposed to bind to the RyR1 receptor through a cluster of basic amino acid residues followed by Ser or Thr.[25] Mca possesses this motif which is located on the surface from which emerges the dipole moment resulting from the electrostatic anisotropy. Such a dipole has been formerly put forward as a guideline for potassium blockers to be correctly oriented towards the potassium channels.[26] We modelled the structure of Iptxa on the basis of the experimentally determined structure of Mca and demonstrated that the dipolar moment of Iptxa also emerges from the basic rich surface of Iptxa. We can therefore propose this basic-rich surface as the interacting surface of Mca as well as of Iptxa (Fig. 6). It is well possible that the activating segment of the dihydropyridine receptor II-III loop adopts a fold in which the basic residues will be organised in a similar fashion, in order to interact with the ryanodine receptor.

CONCLUSION

Structural determination of Mca is the first step in the understanding of the dihydropyridine/ryanodine receptor interaction. The ryanodine receptor's overall shape has been visualised by cryoelectron microscopy and image reconstruction,[27] as well as the complex between RyR1 and Iptxa[4] showing at very low resolution the location of the specific binding site of Iptxa on the architecture of RyR1. This site is composed of a short acidic-rich segment (residues 1076–1112), proposed to be one of the physiological activating sites of RyR1 during excitation-contraction coupling. Over-expression of this domain is under way and will lead to new insights in the structure of the Mca-binding site/Mca complex, designed to mimic the allosteric interaction of dihydropyridine/ryanodyne receptors.

ACKNOWLEDGMENTS

This work is supported in part by the *Association Française contre les Myopathies* . One of us (J-G.R.) is the recipient of a grant from *the Conseil Régional Provence-Alpes Côte d'Azur* (France) associated with *Latoxan* company. The authors would like to thank Dr. Christian Cambillau for constant interest and support.

REFERENCES

1. Franzini-Armstrong C, Protasi F. Ryanodine receptors of striated muscles: a complex channel capable of multiple interactions. Physiol Rev 1997;77:699–729.
2. Leong P, MacLennan DH. The cytoplasmic loops between domains II and III and domains III and IV in the skeletal muscle dihydropyridine receptor bind to a contiguous site in the skeletal muscle ryanodine receptor. J Biol Chem 1998;293:29958–29964.
3. Fajloun Z, Kharrat R, Chen L, et al. Chemical synthesis and characterization of maurocalcine, a scorpion toxin that activates Ca++ release channel/ryanodine receptors. FEBS Lett 2000;469: 179–185.
4. Samso M, Trujillo R, Gurrola GB, Valdivia HH, Wagenknecht T. Three-dimensional location of the imperatoxin A binding site on the ryanodine receptor. J Cell Biol 1999;146:493–499.
5. Marion D, Ikuto M, Tschudin R, Bax A. Rapid recording of 2D NMR spectra without phase cycling. Application to the study of hydrogen exchange in proteins. J Mag Res 1989;85:393–399.
6. Marion D, Wüthrich K. Application of phase sensitive two-dimensional correlated spectroscopy (COSY) for measurements of 1H-1H spin-spin coupling constants in proteins. Biochem Biophys Res Commun 1983;113:967–974.
7. Piotto M, Saudek V, Sklenar V. Gradient-tailored excitation for single-quantum NMR spectroscopy of aqueous solutions. J Biomol NMR 1992;2:661–665.
8. Wüthrich K. In: NMR of proteins and nucleic acids. New York: John Wiley & Sons; 1986:2–199.
9. Bartels C, Xia T-H, Billeter M, Güntert P, Wüthrich K. The program XEASY for computer-supported NMR spectral analysis of biological macromolecules. J Biomol NMR 1995;5:110.
10. Güntert P, Braun W, Wüthrich K. Efficient computation of three dimensional protein structures in solution from NMR data using the programs CALIBA, HABAS and GLOMSA. J Mol Biol1991;217: 517–530.
11. Güntert P, Wüthrich K. Improved efficiency of protein structure calculations from NMR data using the program DIANA with redundent dihedral angle constraints. J Biomol NMR 1991;1:447–456.
12. Szyperski T, Güntert P, Otting G, Wüthrich KJ. Determination of scalar coupling constants by inverse Fourier transformation of in-phase multiplets. Magn Reson 1992;99:552–560.
13. Roussel A, Cambillau C. Silicon graphics geometry partner directory. Mountain View, CA: Silicon Graphics; 1989. p 77–78.
14. Laskowski RA, MacArthur MW, Moss DM, Thornton JM. A program to check the stereochemical quality of protein structures. J Appl Cryst 1993;26:283–291.
15. Nicholls A, Sharp KA, Honig B. Protein folding and association: insights from the interfacial and thermodynamic properties of hydrocarbons. Proteins 1991;11:281–296.
16. Nicholls A, Honig B. A rapid finite difference algorithm, utilizing successive over-relaxation to solve the Poisson-Boltzmann equation. J Comp Chem 1991;12:435–445.
17. Brünger AT, Adams PD, Clore GM, et al. Crystallography and NMR system (CNS): a new software system for macromolecular structure determination. Acta Crystallogr 1998;54:905–921.
18. Pallaghy PK, Nielsen KJ, Craik DJ, Norton RS. Common structural motif incorporating a cystine knot and a triple-stranded beta-sheet in toxic and inhibitory polypeptides. Protein Sci 1994;3: 1833–1839.
19. Wakamatsu K, Kohda D, Hatanaka H, et al. Structure-activity relationships of mu-conotoxin GIIIA: structure determination of active and inactive sodium channel blocker peptides by NMR and simulated annealing calculations. Biochemistry 1992;31:12577–12584.
20. Hill JM, Alewood PF, Craik DJ. Solution structure of the sodium

channel antagonist conotoxin GS: a new molecular caliper for probing sodium channel geometry. Structure 1997;5:571–583.
21. Scanlon MJ, Naranjo D, Thomas L, Alewood PF, Lewis RJ, Craik DJ. Solution structure and proposed binding mechanism of a novel potassium channel toxin kappa-conotoxin PVIIA. Structure 1997; 5:1585–1597.
22. Civera C, Vazquez A, Sevilla JM, et al. Solution structure determination by two-dimensional 1H NMR of omega-conotoxin MVIID, a calcium channel blocker peptide. Biochem Biophys Res Comm 1999;254:32–35.
23. Kim JI, Konishi S, Iwai H, et al. Tyr13 is essential for the binding of omega-conotoxin MVIIC to the P/Q-type calcium channel. J Mol Biol 1995;250:659–671.
24. Zamudio FZ, Gurrola GB, Arevalo C, et al. Primary structure and synthesis of Imperatoxin A (IpTx(a)), a peptide activator of Ca2+ release channels/ryanodine receptors. FEBS Lett 1997;405:385–389.
25. Gurrola GB, Arévalo C, Sreekumar R, Lokuta AJ, Walker JW, Valvidia H. Activation of ryanodine receptors by imperatoxin A and a peptide segment of the II-III loop of the dihydropyridine receptor. J Biol Chem 1999;274:7879–7886.
26. Blanc E, Lecomte C, Van Rietschoten J, Sabatier JM, Darbon H. Solution structure of TsKapa, a charybdotoxin-like scorpion toxin from Tityus serrulatus with high affinity for apamin-sensitive Ca(2+)-activated K+ channels. Proteins 1997;29:359–369.
27. Wagenknecht T, Radermacher M. Ryanodine receptors: structure and macromolecular interactions. Curr Opin Struct Biol 1997;7: 258–265.